

Supporting Information

Gas-water Interface Engineered Exceptional Photoconversion of Fatty Acids to Olefins

Qin Dai^{a,b,§}, Jingyi Lin^{a,b,§}, Hongbin Cao^a, He Zhao^{a,*}, Guangfei Yu^{a,b}, Chaoqun Li^b, Tianyu Wang^c, Yanchun Shi^a, Guangwei Wang^{c,*} and Jinlong Gong^{d,*}

^a National Key Laboratory of Biochemical Engineering, Beijing Engineering Research Center of Process Pollution Control, Institute of Process Engineering, Chinese Academy of Sciences, Beijing 100190, China

^b University of Chinese Academy of Sciences, Beijing 100049, China

^c Department of Chemistry School of Science, Tianjin University, Tianjin 300072, China

^d Key Laboratory for Green Chemical Technology of Ministry of Education, School of Chemical Engineering & Technology, Tianjin University, Collaborative Innovation Center of Chemical Science and Engineering (Tianjin), Tianjin 300072, China

^e Beijing Key Laboratory for Science and Application of Functional Molecular and Crystalline Materials, Department of Chemistry, University of Science and Technology Beijing, Beijing 100083, China

Table of Contents

Fig. S1. Schematic diagram of photoconversion of FAs at the gas-water interface into gaseous hydrocarbons detected by the <i>in-situ</i> GC-MS/FID.	4
Fig. S2. The picture of NA enriched at the gas-water interface.	4
Fig. S3. Gas and liquid products of photoirradiation of NA detected by the <i>in-situ</i> GC-MS/FID.	5
Table S1. The solubility of different FAs in water	5
Fig. S4. Enlarged view of the molecular layer thickness formed by different FAs.	6
Fig. S5. Light spectrum used in the experiment.	6
Fig. S6. <i>In-situ</i> ESR spectrum obtained before and after photoirradiation of NA aqueous, using DMPO as a trapping agent. The position of the adduct signal is marked: (*) DMPO-OH.	7
Fig. S7. (a) High resolution mass spectrometry (HRMS) of generated three carbon radicals after photoirradiation captured by TEMPO detected under positive mode (The positions of the adduct signal were marked), (b) corresponding reaction schemes and molecular formulas of three types of carbon radicals and TEMPO.	8
Fig. S8. The pH of the NA solution varied with photoirradiation time.	9

Fig. S9. Intrinsic reaction coordinate (IRC) results for the C-O fission of NA^* and C-C fission of $[\text{NA}]^*$ complexed with a different number of interfacial water at the B3LYP/6-31G* level. **(a)** NA^* , **(b)** $[\text{NA}/1\text{H}_2\text{O}]^*$ and **(c)** $[\text{NA}/2\text{H}_2\text{O}]^*$; **(d)** $[\text{NA}]^*$, **(e)** $[\text{NA}'/1\text{H}_2\text{O}]^*$ and **(f)** $[\text{NA}'/2\text{H}_2\text{O}]^*$. The distance between the atoms is angstrom. 10

Table S2. Calculated reaction energies at B3LYP /6-311+G (2df, 2p) for the C-O and C-C fission of triplet NA combined with a different number of interfacial water. 11

Table S3. Energies for reactants and products calculated at B3LYP/6-311+G(2df, 2p) level. 12

Table S4. Calculated reaction energies at B3LYP/6-311+G (2df, 2p). 13

Fig. S10. Gaseous hydrocarbon concentration under different gas atmospheres. 14

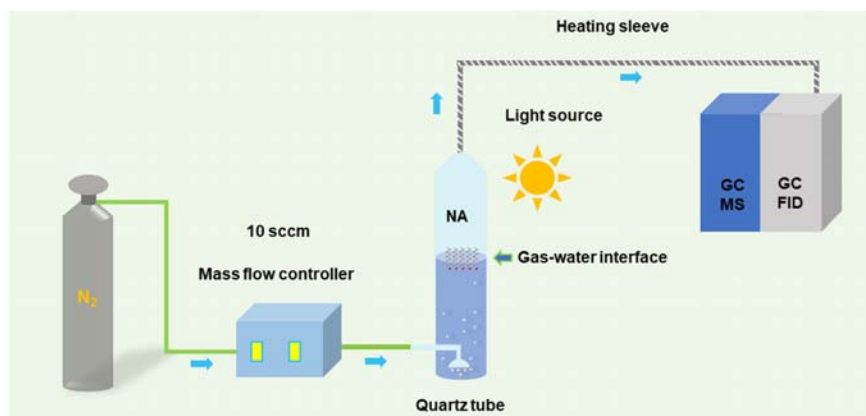


Fig. S1. Schematic diagram of photoconversion of FAs at the gas-water interface into gaseous hydrocarbons detected by the *in-situ* GC-MS/FID.



Fig. S2. The picture of NA enriched at the gas-water interface.

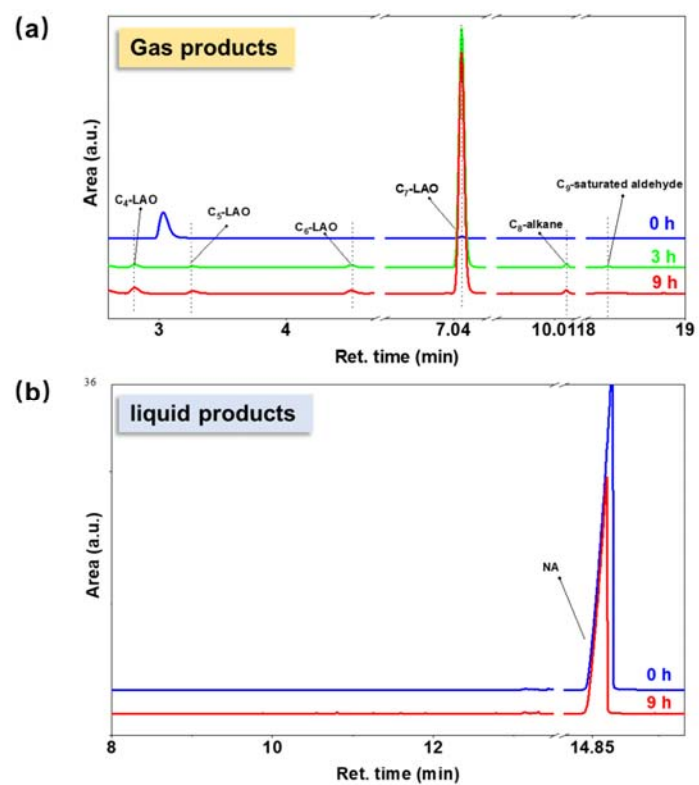


Fig. S3. Gas and liquid products of photoirradiation of NA detected by the *in-situ* GC-MS/FID.

Table S1. The solubility of different FAs in water

Name	Solubility (g/L)	Molecular weight	Solubility (mM)
NA	0.30	158.23	1.90
C ₈ -acid	0.68 (20 °C)	144.21	4.72 (20 °C)
C ₇ -acid	2.80	130.18	21.50
C ₆ -acid	11.00 (20 °C)	116.16	94.83 (20 °C)

Unless otherwise indicated, all data are from general conditions (25 °C, 100 kPa)

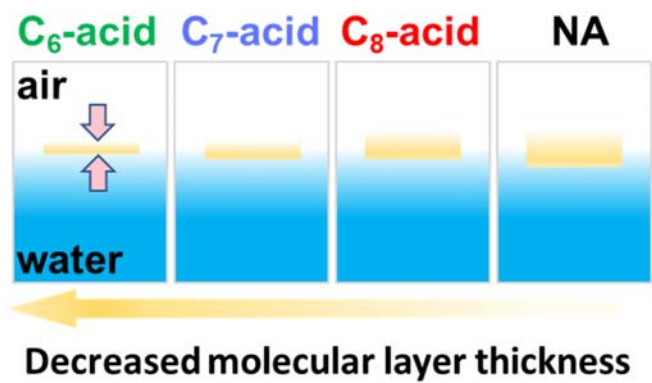


Fig. S4. Enlarged view of the molecular layer thickness formed by different FAs.

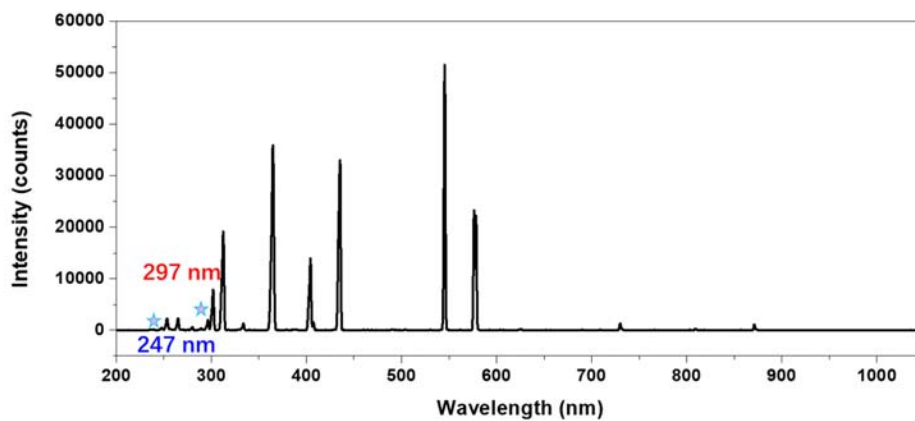


Fig. S5. Light spectrum used in the experiment.

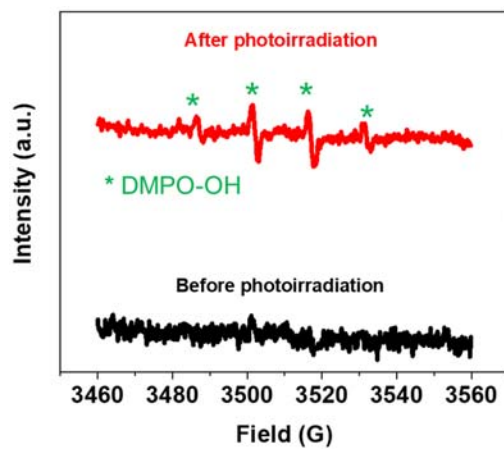


Fig. S6. *In-situ* ESR spectrum obtained before and after photoirradiation of NA aqueous, using DMPO as a trapping agent. The position of the adduct signal is marked: (*) DMPO-OH.

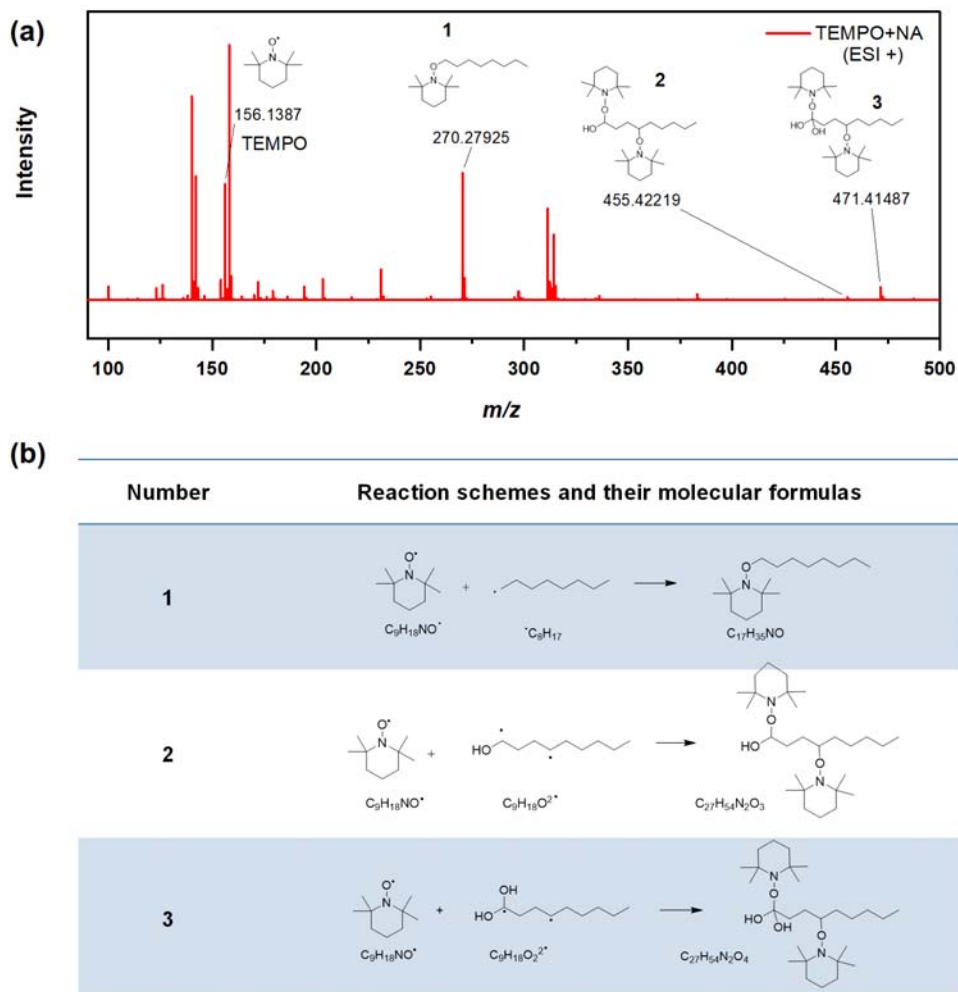


Fig. S7. (a) High resolution mass spectrometry (HRMS) of three carbon radicals captured by TEMPO detected under positive mode (The positions of the adduct signal were marked), **(b)** corresponding reaction schemes and molecular formulas of three types of carbon radicals and TEMPO.

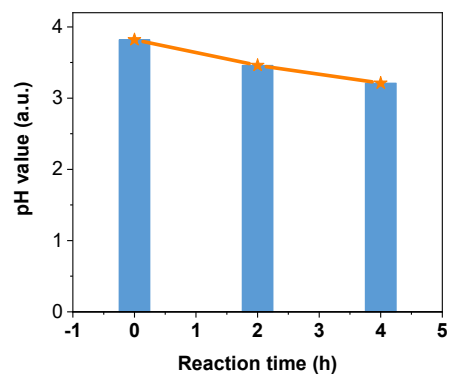


Fig. S8. The pH of the NA solution varied with photoirradiation time.

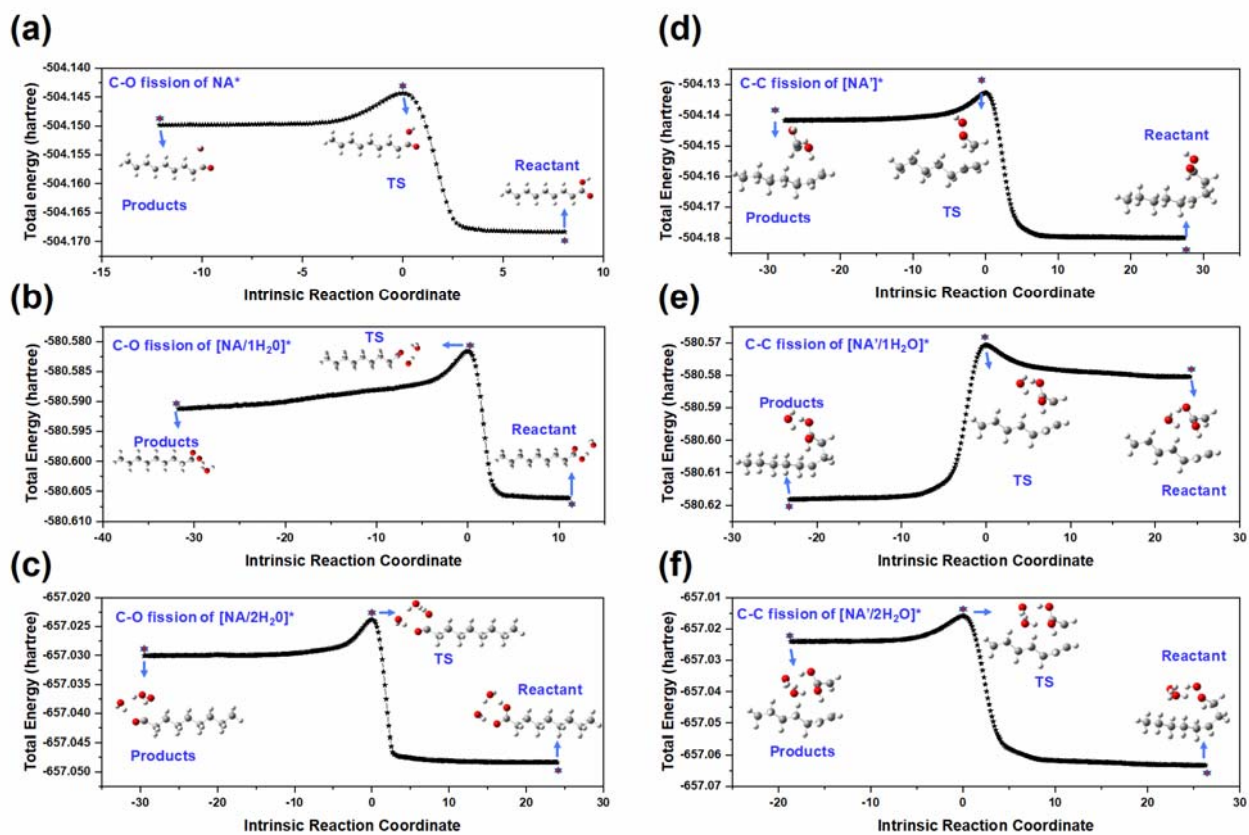


Fig. S9. Intrinsic reaction coordinate (IRC) results for the C-O fission of NA^* and C-C fission of $[\text{NA}']^*$ complexed with a different number of interfacial water at the B3LYP/6-31G* level. **(a)** NA^* , **(b)** $[\text{NA}/1\text{H}_2\text{O}]^*$ and **(c)** $[\text{NA}/2\text{H}_2\text{O}]^*$; **(d)** $[\text{NA}']^*$, **(e)** $[\text{NA}'/1\text{H}_2\text{O}]^*$ and **(f)** $[\text{NA}'/2\text{H}_2\text{O}]^*$. The distance between the atoms is angstrom.

Table S2. Calculated reaction energies at B3LYP /6-311+G (2df, 2p) for the C-O and C-C fission of triplet NA combined with a different number of interfacial water.

(a)

C-O fission					
Name	SP (single point) energy-low (hartree)	Zero-point energy (hartree)	Thermal correction to enthalpy (hartree)	SP energy-high (hartree)	H (298.15K, hartree)
NA	-504.3243362	0.261956	0.276708	-504.5106772	-504.2339692
NA*-reactant	-504.168318	0.258084	0.27351	-504.353726	-504.080216
[NA/1H ₂ O]*-reactant	-580.60611	0.282906	0.301098	-580.835901	-580.534803
[NA/2H ₂ O]*-reactant	-657.048333	0.308271	0.328527	-657.320754	-656.992227
NA*-reactant-TS	-504.144341	0.255218	0.27076	-504.330792	-504.060032
[NA/1H ₂ O]*-TS	-580.581594	0.280516	0.298837	-580.812422	-580.513585
[NA/2H ₂ O]*-TS	-657.023796	0.305499	0.326006	-657.297474	-656.971468
NA*-reactant-products	-504.154905	0.254652	0.271174	-504.342523	-504.071349
[NA/1H ₂ O]*-products	-580.592488	0.27917	0.298683	-580.82479	-580.526107
[NA/2H ₂ O]*-products	-657.030019	0.304104	0.325436	-657.305809	-656.980373

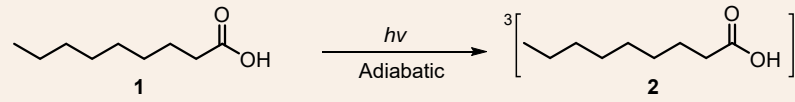
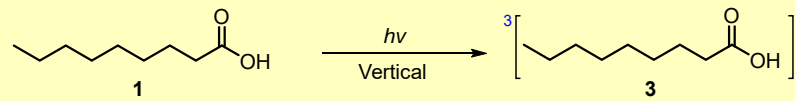
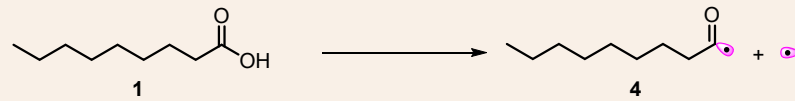
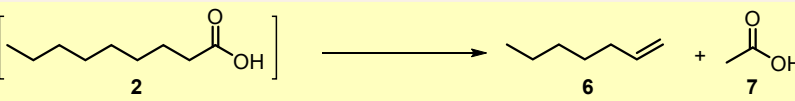
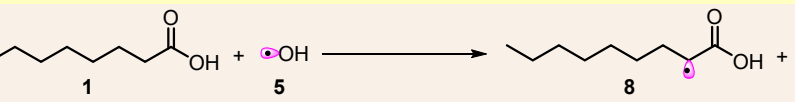
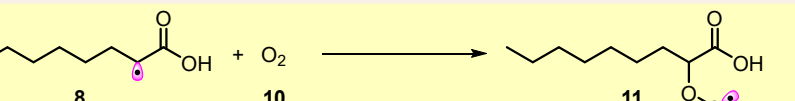
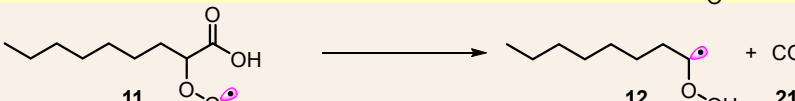
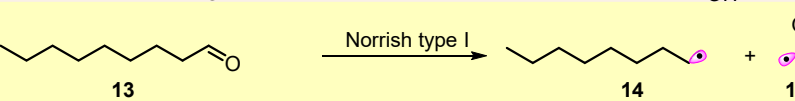
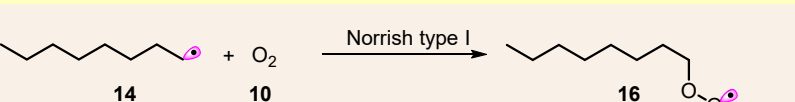
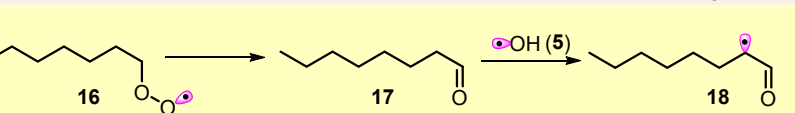

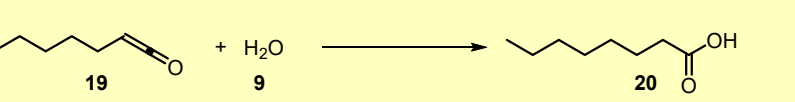
(b)

C-C fission					
Name	SP (single point) energy-low (hartree)	Zero-point energy (hartree)	Thermal correction to Enthalpy (hartree)	SP energy-high (hartree)	H (298.15K, hartree)
NA	-504.3243362	0.261956	0.276708	-504.5106772	-504.2339692
[NA]*	-504.169067	0.258176	0.273284	-504.354159	-504.080875
[NA'/1H ₂ O]*	-580.607159	0.282832	0.300802	-580.836952	-580.53615
[NA'/2H ₂ O]*	-657.048564	0.307816	0.328073	-657.321632	-656.993559
[NA'-radical]*-reactant	-504.180037	0.257526	0.272707	-504.372777	-504.10007
[NA'-radical/1H ₂ O]*-reactant	-580.618163	0.282572	0.300428	-580.854059	-580.553631
[NA'-radical/2H ₂ O]*-reactant	-657.063584	0.308354	0.328163	-657.342106	-657.013943
[NA'-radical]*-TS	-504.132733	0.254029	0.269613	-504.329971	-504.060358
[NA'-radical/1H ₂ O]*-TS	-580.570712	0.27924	0.297378	-580.811074	-580.513696
[NA'-radical/2H ₂ O]*-TS	-657.015889	0.304502	0.3247	-657.298193	-656.973493
[NA'-radical]*-products	-504.141647	0.252906	0.269915	-504.3298193	-504.060358
[NA'-radical/1H ₂ O]*-products	-580.580452	0.278159	0.297773	-580.820446	-580.522673
[NA'-radical/2H ₂ O]*-products	-657.024163	0.30372	0.325371	-657.308186	-656.982815

Table S3. Energies for reactants and products calculated at B3LYP/6-311+G(2df, 2p) level.

Product number	Name	SP (single point) energy-low (hartree)	Zero-point energy (hartree)	Thermal correction to enthalpy (hartree)	SP energy-high (hartree)	H (298.15K, hartree)
1	NA	-504.3243362	0.261956	0.276708	-504.5106772	-504.2339692
2	NA* adiabatic	-504.1683183	0.258084	0.27351	-504.3537263	-504.0802163
3	NA* vertical	-504.1307637	0.256627	0.269152	-504.318766	-504.049614
4	Nonaldehyde radical	-428.4114082	0.243735	0.257743	-428.5627158	-428.3049728
5	.OH	-75.73246773	0.008305	0.01161	-75.77363127	-75.76202127
6	C ₇ -LAO	-275.1858522	0.194655	0.204747	-275.2836247	-275.0788777
7	Acetic acid	-229.097777	0.06149	0.066998	-229.1943078	-229.1273098
8	NA radical	-503.668376	0.248299	0.262946	-503.854315	-503.591369
9	H ₂ O	-76.42269	0.020985	0.024764	-76.47498288	-76.45021888
10	O ₂	-150.2602365	0.003747	0.007055	-150.3200959	-150.3130409
11	NA peroxy radical	-654.034814	0.257808	0.274385	-654.2756133	-654.0012283
12	C ₈ -OOH	-465.490075	0.238801	0.254308	-465.6676423	-465.4133343
13	Nonanal	-429.0663937	0.256513	0.270459	-429.2190232	-428.9485642
14	C ₈ -alkane radical	-315.0679497	0.231574	0.243958	-315.1776556	-314.9336976
15	C ₁ -aldehyde radical	-113.8481123	0.013232	0.017032	-113.8954442	-113.8784122
16	C ₈ -alkane peroxy radical	-465.4568438	0.243479	0.25745	-465.6228393	-465.3653893
17	C ₈ -aldehyde	-389.748298	0.227917	0.240522	-389.8880209	-389.6474989
18	C ₉ -aldehyde-radical	-389.101256	0.215341	0.227621	-389.2394115	-389.0117905
19	C ₈ -aldehyde-two bonds	-388.510915	0.204195	0.216339	-388.6498275	-388.4334885
20	C ₈ -acid	-465.0062629	0.233598	0.246931	-465.1798751	-464.9329441
21	CO ₂	-188.578313	0.011418	0.015015	-188.6542289	-188.6392139

Table S4. Calculated reaction energies at B3LYP/6-311+G (2df, 2p).

#	Reactions	ΔH^0 (298.15 K) (kJ/mol)
(0)	 $1 \xrightarrow[\text{Adiabatic}]{h\nu} {}^3\left[2\right]$	+403.68
(1)	 $1 \xrightarrow[\text{Vertical}]{h\nu} {}^3\left[3\right]$	+484.02
(2)	 $1 \longrightarrow 4 + 5$	+438.39
(3)	 ${}^3\left[2\right] \longrightarrow 6 + 7$	-330.74
(4)	 $1 + 5 \longrightarrow 8 + 9$	-119.72
(5)	 $8 + 10 \longrightarrow 11$	-524.20
(6)	 $11 \longrightarrow 12 + 21$	-134.74
(7)	 $13 \xrightarrow{\text{Norrish type I}} 14 + 15$	+358.26
(8)	 $14 + 10 \xrightarrow{\text{Norrish type I}} 16$	-311.52
(9)	 $16 \longrightarrow 17 + 5 \xrightarrow{\text{OH (5)}} 18 + 9$	-115.87/-137.81
(10)	 $2 \cdot 18 \longrightarrow 17 + 19$	-152.72
(11)	 $19 + 9 \longrightarrow 20$	-129.27

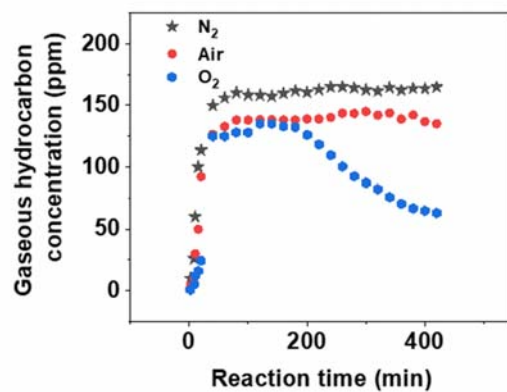


Fig. S10. Gaseous hydrocarbon concentration under different gas atmospheres.